Axial Coordination and Conformational Heterogeneity of Nickel(II) Tetraphenylporphyrin Complexes with Nitrogenous Bases†

Song-Ling Jia,‡,§ Walter Jentzen,‡,§,|| Mayou Shang,⊥ Xing-Zhi Song,‡,§ Jian-Guo Ma,‡,§ W. Robert Scheidt,⊥ and John A. Shelnutt*,‡,§

Materials Theory and Computation Department, Sandia National Laboratories, Albuquerque, New Mexico 87185-1349, Department of Chemistry, University of New Mexico, Albuquerque, New Mexico 87131, Klinik und Poliklinik für Nuklearmedizin, Universität GH Essen, Hufelandstrasse 55, D-45147 Essen, Germany, and Department of Chemistry and Biochemistry, University of Notre Dame, Notre Dame, Indiana 46556

Received March 13, 1998

Axial ligation of nickel(II) 5,10,15,20-tetraphenylporphyrin (NiTPP) with pyrrolidine or piperidine has been investigated using X-ray crystallography, UV−visible spectroscopy, resonance Raman spectroscopy, and molecular mechanics (MM) calculations. By varying the pyrrolidine concentration in dichloromethane, distinct ν_4 Raman lines are found for the four-, five-, and six-coordinate species of NiTPP. The equilibrium constants for addition of the first and second pyrrolidine axial ligands are 1.1 and 3.8 M^{-1}, respectively. The axial ligands and their orientations influence the type and magnitude of the calculated nonplanar distortion. The differences in the calculated energies of the conformers having different ligand rotational angles are small so they may coexist in solution. Because of the similarity in macrocyclic structural parameters of these conformers and the free rotation of the axial ligands, narrow and symmetric ν_2 and ν_8 Raman lines are observed. Nonetheless, the normal-coordinate structural-decomposition analysis of the nonplanar distortions of the calculated structures and the crystal structure of the bis(piperidine) complex reveals a relationship between the orientations of axial ligand(s) and the macrocyclic distortions. For the five-coordinate complex with the plane of the axial ligand bisecting the $Ni-N_{pyrrole}$ bonds, a primarily ruffled deformation results. With the ligand plane eclipsing the $Ni-N_{pyrrole}$ bonds, a mainly saddled deformation occurs. With the addition of the second axial ligand, the small doming of the five-coordinate complexes disappears, and ruffling or saddling deformations change depending on the relative orientation of the two axial ligands. The crystal structure of the NiTPP bis(piperidine) complex shows a macrocycle distortion composed of *wav*(*x*) and *wav*(*y*) symmetric deformations, but no ruffling, saddling, or doming. The difference in the calculated and observed distortions results partly from the phenyl group orientation imposed by crystal packing forces. MM calculations predict three stable conformers (*ruf*, *sad*, and planar) for four-coordinate NiTPP, and resonance Raman evidence for these conformers was given previously.

Introduction

The possible functional significance of nonplanar heme distortions in proteins is becoming a more and more compelling question.[1−11] This was first brought to light when it was noticed that the nonplanar distortions of the iron−porphyrin (heme) cofactor are conserved for all of the high-resolution crystal structures of mitochondrial cytochromes *c*.[1−4,10,11] Recently, an analysis using normal-coordinate structural decomposition (NSD) of the more than 800 heme groups in protein crystal structures convincingly showed that the nonplanarity of the porphyrin is conserved for many types of proteins.[10,11] It is also now evident that the protein must provide the distortion energy required to make the heme group nonplanar, since in solution the heme is nearly planar.[12] Furthermore, it is clear that the type and degree of nonplanar distortion depends on the fine points of the protein−heme interaction. Hydrogen bonds,

† Sandia is a multiprogram laboratory operated by Sandia Corporation, a Lockheed Martin Company, for the United States Department of Energy under Contract DE-AC04-94AL85000. Work at Notre Dame University was supported by NIH Grants GM-38401 and RR-06709.

* To whom correspondence should be addressed.
‡ Sandia National Laboratories.
§ University of New Mexico
|| Universität GH Essen.
⊥ University of Notre Dame.

(1) Shelnutt, J. A.; Song, X.-Z.; Ma, J.-G.; Jia, S.-L.; Jentzen, W.; Medforth, C. J. *Chem. Soc. Rev*. **1998**, *27*, 31.
(2) Hobbs, J. D.; Shelnutt, J. A. *J. Protein Chem*. **1995**, *14*, 19.
(3) Ma, J.-G.; Laberge, M.; Song, X.-Z.; Jentzen, W.; Jia, S.-L.; Zhang, J.; Vanderkooi, J. M.; Shelnutt, J. A. *Biochemistry* **1998**, *37*, 5118.
(4) Martinez, S. E.; Smith, J. L.; Huang, D.; Szczepaniak, A.; Cramer, W. A. In *Research in Photosynthesis*; Murata, N., Ed.; Proceedings of the IXth International Congress on Photosynthesis; Kluwer Academic: Dordrecht, The Netherlands, 1992; Vol. 2, p 495.
(5) Alden, R. G.; Ondrias, M. R.; Shelnutt, J. A. *J. Am. Chem. Soc*. **1990**, *112*, 691.
(6) Hobbs, J. D.; Majumder, S. A.; Luo, L.; Sickelsmith, G. A.; Quirke, J. M. E.; Medforth, C. J.; Smith, K. M.; Shelnutt, J. A. *J. Am. Chem. Soc*. **1994**, *116*, 3261.
(7) Barkia, K. M.; Chantranupong, L.; Smith, K. M.; Fajer, J. *J. Am. Chem. Soc*. **1988**, *110*, 7566.
(8) Waditschatka, R.; Kratky, C.; Juan, B.; Heinzer, J. Eschenmoser, A. *J. Chem. Soc., Chem. Commun*. **1985**, 1604.
(9) Kadish, K. M.; Caemelbecke, E. V.; Boulas, P.; D'Souza, F. D.; Vogel, E.; Kisters, M.; Medforth, C. J.; Smith, K. M. *Inorg. Chem*. **1993**, *32*, 4177.
(10) Jentzen, W.; Song, X.-Z.; Shelnutt, J. A. *J. Phys. Chem. B* **1997**, *101*, 1684.
(11) Jentzen, W.; Ma, J.-G.; Shelnutt, J. A. *Biophys. J*. **1998**, *74*, 753.
(12) Sparks, L. D.; Medforth, C. J.; Park, M.-S.; Chamberlain, J. R.; Ondrias, M. R.; Senge, M. O.; Smith, K. M.; Shelnutt, J. A. *J. Am. Chem. Soc*. **1993**, *115*, 581.

S0020-1669(98)00289-4 CCC: $15.00
Published on Web 07/31/1998

the covalent linkage between the heme and protein, and the steric interactions between protein and heme are important in causing the nonplanar distortions.[13] For the present work, the heme interaction with axial ligands is the focus. The specific interaction between the axial histidine ligands and the heme is known to alter the oxidation potentials and spectroscopic properties of cytochromes.[14] Correlations between the orientation of the planes of the axial ligands and redox potential have been proposed.[15−18] To elucidate the effects of axial ligation on macrocyclic nonplanarity, the coordination complexes of a well-characterized model compound, nickel(II) tetraphenylporphyrin (NiTPP), are investigated herein.[19]

The combination of X-ray crystallography, resonance Raman spectroscopy, and molecular mechanics (MM) calculations has been used to investigate the nonplanar distortions of synthetic porphyrins without axial ligands.[13,20−24] In this case, the type and degree of nonplanar distortion is determined by the central metal and the peripheral substituents of the porphyrin. As a model for the conserved ruffling of the heme of mitochondrial cytochromes *c*, a series of nickel(II) meso-tetrasubstituted porphyrins were investigated, and the lowest-energy structures for these porphyrins are found to be ruffled because of the $\alpha\beta\alpha\beta$ orientation of the substituent groups.[13] Similarly, a series of nickel(II) 5,15-disubstituted porphyrins are found to adopt a gabled or roof conformation, thus serving as a model for the distortion of the hemes in the α-chains of human deoxyhemoglobin A.[22] UV−visible absorption and resonance Raman spectroscopy have proved effective in addressing questions concerning the state of axial ligation and out-of-plane distortion of these porphyrins. In particular, the Raman core-size and oxidation-state marker lines, ν_2, ν_3, ν_4, ν_8, ν_{10}, are good structural indicators.[20−29] UV−visible absorption spectroscopy also provides information about axial ligation state and nonplanar distortion. For example, both axial ligation and distortion cause a red shift of the Soret absorption band for nickel porphyrins.[30−34] In spite of these successful studies, suitable spectroscopic markers for porphyrin distortion are lacking, especially for axial coordination complexes.

NiTPP is a common model metalloporphyrin that is known to form axial coordination complexes with nitrogenous bases like pyridine and piperidine. It has been claimed that both five- and six-coordinate complexes coexist in strong coordinating solvents like piperidine,[30−34] although the five-coordinate species has not been observed directly. In this study, we measured the resonance Raman spectra of NiTPP in dichloromethane solution with different pyrrolidine concentrations, and as in previous studies we observe only four-coordinate species in neat dichloromethane and six-coordinate species at high concentrations of pyrrolidine. However, a distinct ν_4 Raman line for the five-coordinate NiTPP−pyrrolidine complex is identified in the low concentration range where, based on the measured equilibrium association constants, its concentration is sufficient to be observed. In addition, the resonance Raman data indicate an apparent decrease in macrocyclic conformational heterogeneity resulting from axial coordination. This is at variance with MM calculations and NSD analyses of the energy-minimized conformers of five-and six-coordinate NiTPP complexes, which indicate many coexisting conformers differing in the orientations of the axial ligand(s) and in the nonplanar distortion of the porphyrin macrocycle. An X-ray crystal structure of the bis(piperidine) NiTPP complex verifies that the magnitudes of the calculated distortions are similar to that observed in the crystal. Together, these results place an upper bound on axial ligand contributions to the out-of-plane distortion of hemes in proteins.

Materials and Methods

Materials. Nickel(II) *meso*-tetraphenylporphyrin was obtained from Porphyrin Products, Inc. Dichloromethane, piperidine, and pyrrolidine were of the highest purity available from Aldrich and used as received.

X-ray Crystal Structure Determination. Single-crystal crystallographic experiments were carried out on an Enraf-Nonious FAST area detector diffractometer at 130 K by methods and procedures for small molecules standard in this lab.[35−38] Visual investigation of the $NiTPP(Pip)_2$ crystals under a microscope showed signs of partial facial decomposition. The best crystal was used for data collection and had a refined effective mosaic spread of 2.26°. A brief summary of determined parameters is given in Table 1. A total of 8062 reflections were collected of which 4452 were unique and intensities of 2608 unique reflections were larger than $2.0\sigma(I)$. All reflections were reduced using Lorentz−polarization factors. Isomorphism was assumed on the basis of the similarities of the cell parameters and the complex composition to those of its analog $CoTPP(Pip)_2$.[37] Coordinates of all non-hydrogen atoms were directly taken from the Co analog. After all these non-hydrogen atoms were refined to converge anisotropically,[39] a difference Fourier map showed part of the hydrogen atoms. However,

(13) Jentzen, W.; Simpson, M. C.; Hobbs, J. D.; Song, X.; Ema, T.; Nelson, N. Y.; Medforth, C. J.; Smith, K. M.; Veyrat, M.; Mazzanti, M.; Ramasseul, R.; Marchon, J.-C.; Takeuchi, T.; Goddard, W. A., III; Shelnutt, J. A. *J. Am. Chem. Soc.* **1995**, *117*, 11085.
(14) Gentemann, S.; Medforth, C. J.; Ema, T.; Nelson, N. Y.; Smith, K. M.; Fajer, J.; Holten, D. *Chem. Phys. Lett.* **1995**, *245*, 441.
(15) Walker, F. A.; Huynh, B. H.; Scheidt, W. R.; Osvath, S. R. *J. Am. Chem. Soc*. **1986**, *108*, 5288.
(16) Walker, F. A.; Simonis, U. *J. Am. Chem. Soc.* **1991**, *113*, 8652.
(17) Safo, M. K.; Gupta, G. P.; Walker, F. A.; Scheidt, W. R. *J. Am. Chem. Soc*. **1991**, *113*, 5497.
(18) Safo, M. K.; Walker, F. A.; Raitsimring, A. M.; Walters, W. P.; Dolata, D. P.; Debrunner, P. G.; Scheidt, W. R. *J. Am. Chem. Soc*. **1994**, *116*, 7760.
(19) Jentzen, W.; Unger, E.; Song, X.-Z.; Jia, S.-L.; Turowska-Tyrk, I.; Schweitzer-Stenner, R.; Dreybrodt, W.; Scheidt, W. R.; Shelnutt, J. A. *J. Phys. Chem. A* **1997**, *101*, 5789.
(20) Shelnutt, J. A.; Medforth, C. J.; Berber, M. D.; Barkigia, K. M.; Smith, K. M. *J. Am. Chem. Soc*. **1991**, *113*, 4077.
(21) Shelnutt, J. A.; Majumder, S. A.; Sparks, L. D.; Hobbs, J. D.; Medforth, C. J.; Senge, M. O.; Smith, K. M.; Miura, M.; Quirke, J. M. E. *J. Raman Spectrosc*. **1992**, *23*, 523.
(22) Song, X.-Z.; Jentzen, W.; Jia, S.-L.; Jaquinod, L.; Nurco, D. J.; Marchon, J.-C.; Smith, K. M.; Shelnutt, J. A. *J. Am. Chem. Soc*. **1996**, *118*, 12975.
(23) Song, X.-Z.; Jaquinod, L.; Jentzen, W.; Nurco, D. J.; Jia, S.-L.; Khoury, R. G.; Ma, J.-G.; Medforth, C. J.; Smith, K. M.; Shelnutt, J. A. *Inorg. Chem*. **1998**, *37*, 2009.
(24) Song, X.-Z.; Jentzen, W.; Jaquinod, L.; Khoury, R. G.; Medforth, C. J.; Jia, S.-L.; Ma, J.-G.; Smith, K. M.; Shelnutt, J. A. *Inorg. Chem*. **1998**, *37*, 2117.
(25) Spaulding, L. D.; Chang, C. C.; Yu, N.-T.; Felton, R. H. *J. Am. Chem. Soc*. **1975**, *97*, 2517.
(26) Spiro, T. G. In *Iron Porphyrins*, Part II; Lever, A. B. P.; Gray, H. B., Eds.; Addison-Wesley: Reading, MA, 1982; p 89.
(27) Yamamoto, T.; Palmer, G.; Gill, D.; Salmeen, I. T.; Rimai, L. *J. Biol. Chem*. **1973**, *248*, 5211.
(28) Spiro, T. G.; Strekas, T. C. *J. Am. Chem. Soc*. **1974**, *96*, 338.
(29) Spiro, T. G.; Burke, J. M. *J. Am. Chem. Soc*. **1976**, *98*, 5482.
(30) McLees, D. D.; Caughey, W. S. *Biochemistry* **1968**, *7*, 642.
(31) Abraham, R. J.; Swinton, P. F. *J. Chem. Soc. B* **1969**, *8*, 903.
(32) La Mar, G. N.; Walker, F. A. In *The Porphyrins*; Dolphin, D.; Ed.; Academic: New York, 1978; Vol. 4, p 61.
(33) Kim, D.; Spiro, T. G. *J. Am. Chem. Soc*. **1986**, *108*, 2099.
(34) Kim, D.; Su, Y. O.; Spiro, T. G. *Inorg. Chem*. **1986**, *25*, 3988. (The ν_{29} line for both five-coordinate and six-coordinate forms of NiTPP might appear at nearly the same position. The assignment for the line at 1359 cm^{-1} to ν_{29} (not ν_{28} as claimed by Kim et al.) is based on the normal coordinate analysis by Li et al.[41−43] According to Li et al., ν_{29} is close to ν_4, but ν_{28} is between ν_3 and ν_2.
(35) Scheidt, W. R.; Turowska-Tyrk, I. *Inorg. Chem*. **1994**, *33*, 1314.
(36) Scheidt, W. R.; Cunningham, J. A.; Hoard, J. L. *J. Am. Chem. Soc*. **1973**, *95*, 8289.
(37) Scheidt, W. R. *J. Am. Chem. Soc*. **1974**, *96*, 84.
(38) Lauher, J. W.; Ibers, J. A. *J. Am. Chem. Soc*. **1974**, *96*, 4447.

Table 1. Crystallographic Data

molecule	Ni(TPP)(Pip)$_2$
empirical formula	$C_{54}H_{48}N_6Ni$
fw, amu	839.69
crystal system	triclinic
space group	$P\bar{1}$
a, Å	11.065(9)
b, Å	11.885(6)
c, Å	9.7397(8)
α, deg	104.881(4)
β, deg	114.564(4)
γ, deg	101.608(4)
volume, Å^3	1054.5(10)
Z	1
μ, mm^{-1}	0.506
temp, K	130(2)
final *R* indices [$I > 2\sigma(I)$]	$R_1 = 0.0835$, $wR_2 = 0.1725$
R indices (all data)	$R_1 = 0.1575$, $wR_2 = 0.2226$
goodness-of-fit on F^2	0.998

these hydrogen atoms were included in the final refinement only as idealized riding atoms along with the remaining hydrogen atoms whose positional parameters were generated theoretically (C−H = 0.95 Å for R_2CH and 0.99 Å for R_2CH_2). The structure was refined against F^2 by the SHELXL-93 program.[39] The refinement converged to final values of $R_1 = 0.0835$ and $wR_2 = 0.1725$ for observed unique reflections ($I \geq 2.0\sigma(I)$) and $R_1 = 0.1575$ and $wR_2 = 0.2226$ for all unique reflections including those with negative intensities. The weighted *R* factors, wR, are based on F^2 and conventional *R* factors, *R*, on *F*, with *F* set to zero for negative intensities. All reflections, including those with negative intensities, were included in the refinement and the $I \geq 2.0\sigma(I)$ criterion was used only for calculating R_1. The maximum and minimum residual electron densities on the final difference Fourier map were 0.621 and −1.020 e/Å^3, respectively. Final atomic coordinates are listed in Table S2 in the Supporting Information.

Resonance Raman Spectroscopy. Resonance Raman spectra of pairs of porphyrin solutions were obtained simultaneously by using a dual-channel spectrometer described previously.[40] The spectrometer slits were adjusted to obtain a 2−6 cm^{-1} spectral resolution. Two different porphyrin solutions were added to each side of a dual-compartment quartz cell. The reference solution was NiTPP in neat dichloromethane (CH_2Cl_2), and the sample solutions were NiTPP in dichloromethane with different amounts of pyrrolidine. The 413.1-nm line of a krypton ion laser (Coherent, INNOVA 20) was used as the excitation source. The scattering light was collected at 90° to the direction of propagation and polarization of the exciting laser beam. The typical laser power was 50−60 mW. The partitioned cell was rotated at 50 Hz to avoid local heating and to probe alternatively the sample and reference solutions. Polarized spectra were measured by passing the scattered light through a Polaroid sheet oriented parallel or perpendicularly to the polarization direction of the incident beam, followed by a scrambler in front of the spectrometer entrance slit.

UV−Visible Absorption Spectroscopy. The absorption spectra were obtained by using an HP 8452A diode array spectrophotometer (Hewlett-Packard) and 5-mm path length quartz cell. The absorption spectra of porphyrin solutions were taken in dichloromethane, pyrrolidine, and mixtures of the two solvents.

Molecular Mechanics (MM) Calculations. Classical molecular mechanics calculations were performed using POLYGRAF software (Molecular Simulations, Inc.) and a force field developed and modified by Shelnutt et al.[20−24] The force field was originally formulated on the basis of recent normal-coordinate analyses of nickel porphyrins[41−43] and the DREIDING II force field.[44] Force constants for the bond stretches, bond angle bends, bond torsions, and inversions of the porphyrin macrocycle were taken from the normal coordinate analyses of NiOEP. Equilibrium bond distances were varied by least-squares methods until the energy-minimized structure of NiOEP optimally matched the near-planar NiOEP crystal structures. In this optimization procedure, the equilibrium Ni−N bond length was held constant at the known value of 1.855 Å.[20] The most significant recent improvement to the original force field is a reduction in the out-of-plane force constants of Li et al.[41] by 50% so that a difficult set of nonplanar porphyrin strucures were accurately predicted. This set of porphyrins includes NiOEP (both planar and *ruf* conformers), NiTPP (planar and *ruf*), NidPP (planar and *ruf*), NidiPrP (*gab*), NidTBuP (*gab*), free base dodecaphenylporphyrin-F_{28} (*wav*), and Ni tetraisopropylporphyrin (*ruf*). For high-spin and axially ligated nickel, the equilibrium Ni−N bond length was set to 2.07 Å, which was obtained by varying the equilibrium Ni−N bond length until the crystal structure of Ni tetra(*N*-methylpyridinium)porphyrin bis(imidazole) complex was matched by the energy-optimized structure. The parameters for the nickel−nitrogen(ligand) bond length were taken to be the same as for the nickel−nitrogen(pyrrole) bond. The van der Waals parameter for high-spin and axially ligated nickel was taken to be the same as for zinc, obtained from the DREIDING II force field.[12] The torsion for rotation about the Ni−N_{ligand} bond was set to zero.

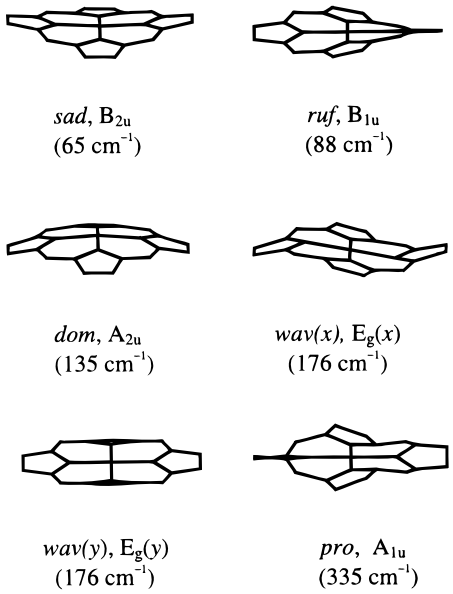

Figure 1. Illustration of the minimum basis set: the lowest-frequency out-of-plane eigenvectors in the Cartesian space and the out-of-plane normal distortions used in describing the nonplanar deformation of the porphyrin macrocycle.

Normal-Coordinate Structural Decomposition (NSD). The energy-minimized and crystallographic structures were anayzed using a new normal-coordinate structural decomposition method to quantify the magnitudes and types of out-of-plane macrocyclic distortions.[10,11] The NSD method characterizes the conformation in terms of equivalent displacements (normal deformations) along the normal coordinates of the D_{4h} symmetric porphyrin macrocycle. This is rigorously possible if the complete set of the out-of-plane normal coordinates is used. However, static distortions of the porphyrin macrocycle predominately occur along the softest (lowest frequency) normal modes.[13] Thus, the most important contributors to the nonplanar distortion are the lowest-frequency out-of-plane coordinates of each symmetry type (B_{1u}, B_{2u}, A_{2u}, E_g, and A_{1u}) illustrated in Figure 1. Adding up the projections of

(39) Programs used in this study included SHELXS-86 (Sheldrick, G. M. *Acta Crystallogr., Sect. A* **1990**, *46*, 467); SHELXL-93 (Sheldrick, G. M. *J. Appl. Crystallogr.*, in preparation), and local modifications of Johnson's ORTEP2. Scattering factors were taken from *International Tables for Crystallography*; Wilson, Ed.; Kluwer Academic Publishers: Dordrecht, 1992; Vol. C.
(40) Shelnutt, J. A. *J. Phys. Chem.* **1983**, *87*, 605.
(41) Li, X.-Y.; Czernuszewics, R. S.; Kincaid, P.; Spiro, T. G. *J. Am. Chem. Soc.* **1989**, *111*, 7012.
(42) Li, X.-Y.; Czernuszewics, R. S.; Kincaid, J. R.; Su, Y. O.; Spiro, T. G. *J. Phys. Chem.* **1990**, *94*, 31.
(43) Li, X.-Y.; Czernuszewics, R. S.; Kincaid, J. R.; Stein, P.; Spiro, T. G. *J. Phys. Chem.* **1990**, *94*, 47.
(44) Mayo, S. L.; Olafson, B. D.; Goddard, W. A., III. *J. Phys. Chem.* **1990**, *94*, 88.

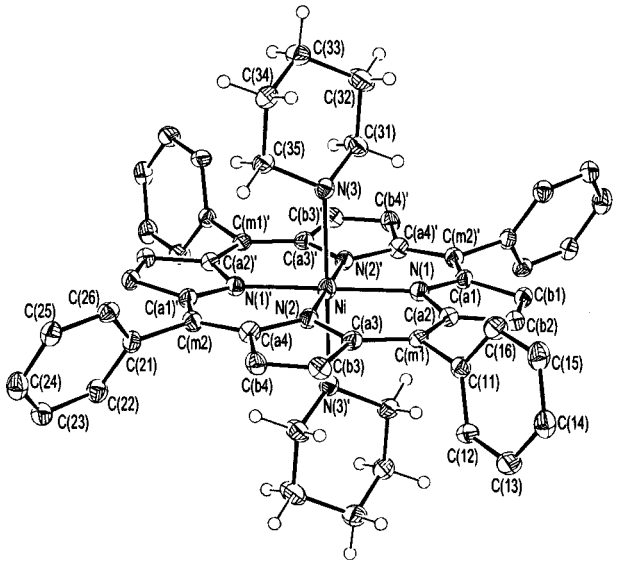

Figure 2. ORTEP drawing of the bis(piperidine) NiTPP molecule.

the total distortion along only these normal coordinates typically simulates the actual distortion accurately. In the present study, only the deformations along these lowest-frequency normal modes are given for the normal-coordinate structural decompositions.

Results

X-ray Crystallography. The crystal structure of bis(piperidine)nickel(II) *meso*-tetraphenylporphyrin and the labeling scheme for the atoms are shown in Figure 2 and in Figures S1 and S2 of the Supporting Information. The crystallographic data and information about the structural determination are listed in Tables 1 and S1. In Tables S2−S6 are given atomic coordinates, structural parameters, and anisotropic displacement parameters.

The average Ni−$N_{pyrrole}$ bond distance for NiTPP(Pip)$_2$ is 2.043 Å, falling in the range between 2.04 and 2.07 Å for the known high-spin six-coordinate nickel(II) derivatives.[45−48] For instances, the Ni−$N_{pyrrole}$ distance for bis(imidazole)nickel(II) tetra(4-*N*-methylpyridyl)porphyrin (NiTMPyP(Im)$_2$) is 2.038 Å.[45] The Ni−N bond lengths are almost equal for the two directions in the porphyrin. The axial Ni−N bond distance is about 0.1 Å longer than NiTMPyP(Im)$_2$ (2.256 compared to 2.160 Å for the bis(imidazole)complex.[45] The expanded core and long axial bond distance are expected because of the electronic configuration for high-spin nickel(II), in which an electron is found in d_{z^2} and $d_{x^2-y^2}$. It is also interesting to compare the series of bis(piperidine) complexes of MTPP(Pip)$_2$, M = Fe(II),[49] Co(III),[36] and Co(II).[37] In the Fe(II) and Co(III) derivatives, which have both empty $d_{x^2-y^2}$ and d_{z^2} orbitals, axial bonds are short and the radius of the porphinato core is ∼2.00 Å. For the cobalt(II) derivative, in which the d_{z^2} orbital is now singly occupied, there is a substantial increase in the axial ligand distances but not in the size of the central core. In the nickel(II) case, as already described, both core expansion and elongation of the axial bonds occurs.

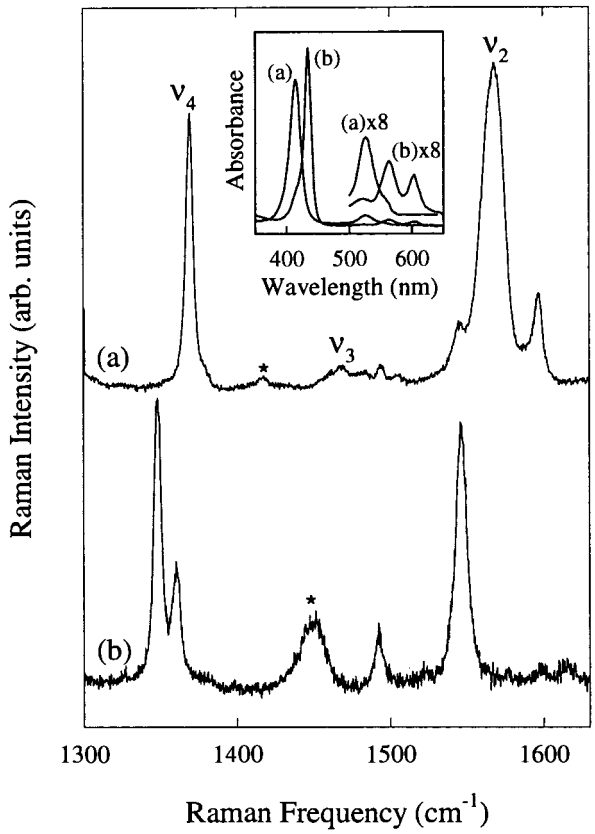

Figure 3. Comparison of resonance Raman spectra for NiTPP in dichloromethane (a) and pyrrolidine (b) in high-frequency region at 413.1-nm excitation. The solvent line is marked with an asterisk (*). Inset is UV−visible absorption spectra for NiTPP in dichloromethane (a) and pyrrolidine (b).

For the crystal structure of NiTPP(Pip)$_2$, the phenyl substituents are not vertical relative to porphyrin macrocycle. Two adjacent phenyl groups tilt to one direction and the other two tilt to the opposite direction so that two opposite phenyl rings eclipse. The dihedral angles between the planes of the two structural classes of phenyl groups and the porphyrin mean plane are 64.9 and 82.5°. Similar phenyl orientations have been observed for Co(III)TPP(Pip)$_2^+$ by Scheidt et al.[37] The axial piperidine ligands are almost perpendicular to porphyrin macrocycle (N_{ax}−Ni−$N_{pyrrole}$ = 90.7, 90.8). The two axial ligands bisect Ni−$N_{pyrrole}$ bonds and are anti-parallel to each other with the protons on the piperidine nitrogen atoms pointing to opposite directions.

Resonance Raman Spectroscopy. Figure 3 is an overview of resonance Raman spectra of NiTPP in the noncoordinating solvent CH_2Cl_2 and in the coordinating solvent pyrrolidine in the region of the structure-sensitive lines. The assignment, labeling, and symmetry of the Raman lines are based on the normal mode analysis.[41−43] It is well known that structure-sensitive skeletal modes ν_2, ν_3, ν_4, and ν_8 are enhanced at 413.1-nm excitation wavelength.[13,20−24,27,50,51] As can be seen from Figure 3, the frequencies of ν_2, ν_3, and ν_4 are obviously much lower in the coordinating solvent. Since the pyrrolidine line near 1450 cm^{-1} obscures ν_3, we focus our attention mainly on the behavior of the skeletal modes ν_2, ν_4, and also the low-frequency mode ν_8.

Figure 4a and b shows resonance Raman spectra for NiTPP in CH_2Cl_2 with different pyrrolidine concentrations. ν_4, which

(45) Kirner, J. F.; Garofalo, J., Jr.; Scheidt, W. R. *Inorg. Nucl. Chem. Lett.* **1975**, *11*, 107.
(46) Balch, A. L.; Olmstead, M. M.; Phillips, S. L. *Inorg. Chem.* **1993**, *32*, 3931.
(47) Ozette, K.; Leduc, P.; Palacio, M.; Bartolic, J.-F.; Barkigia, K. M.; Fajer, J.; Battioni, P.; Mansuy, D. *J. Am. Chem. Soc.* **1997**, *119*, 6442.
(48) Duval, H.; Bulach, V.; Fischer, J.; Weiss, R. *Acta Crystallogr., Sect. C* **1997**, *53*, 10270.
(49) Radonovich, L. J.; Bloom, A.; Hoard, J. L. *J. Am. Chem. Soc.* **1972**, *94*, 2073.
(50) Yamaguchi, H.; Nakano, M.; Itoh, K. *Chem. Lett.* **1982**, 1397.
(51) Parthasarathi, N.; Hansen, C.; Yamaguchi, S.; Spiro, T. G. *J. Am. Chem. Soc.* **1987**, *109*, 3865.

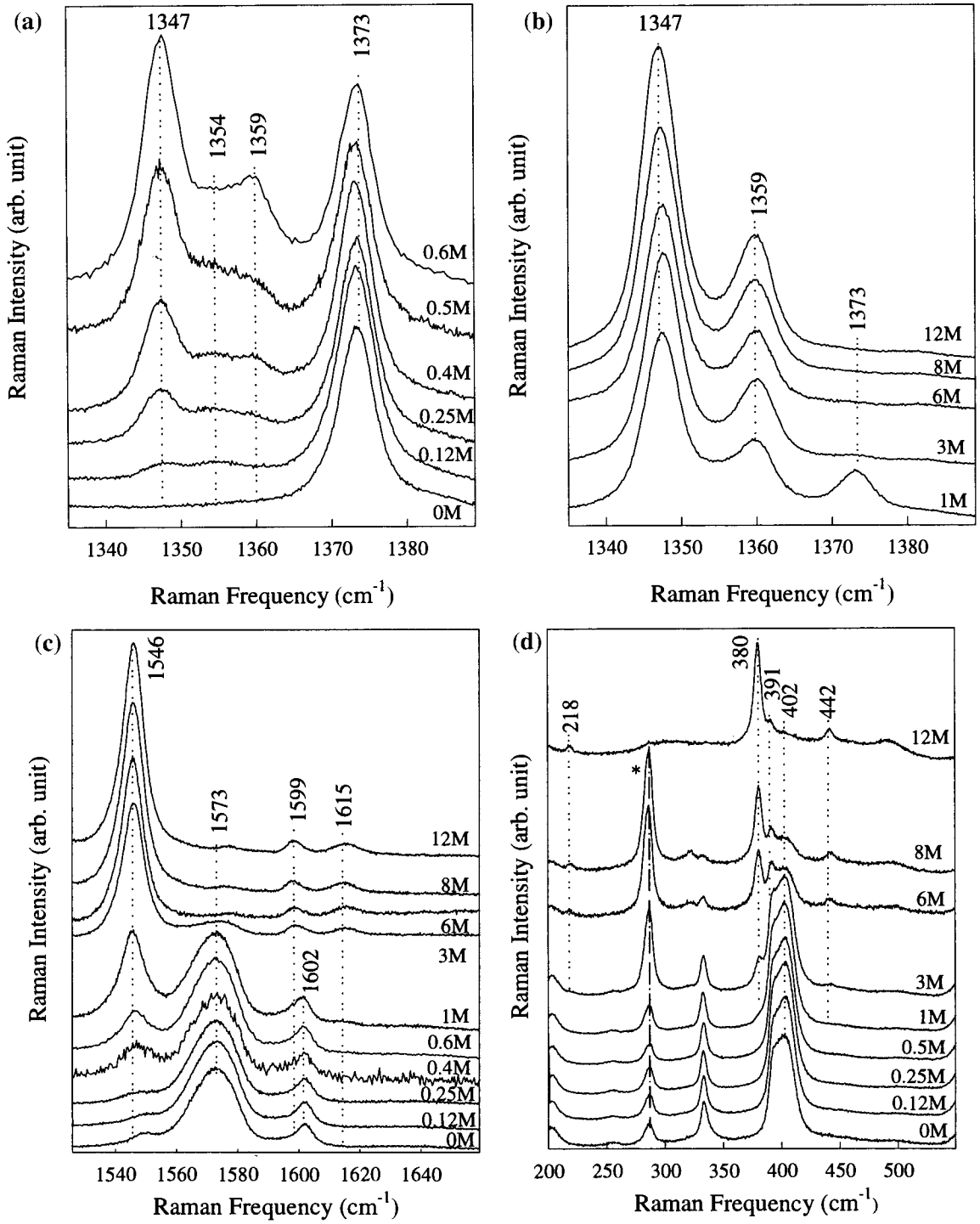

Figure 4. Resonance Raman spectra for NiTPP in dichloromethane with different pyrrolidine concentration in the frequency region 1330−1390 cm^{-1} (a, b), 1500−1660 cm^{-1} (c), and 200−550 cm^{-1} (d) at 413.1-nm excitation. The solvent line is marked with an asterisk (*).

is sensitive to both spin-state and π-electron density for metal tetraphenylporphyrins,[51] is at 1373 cm^{-1} for four-coordinate NiTPP in neat CH_2Cl.[43] As pyrrolidine is added new lines appear in this region of the Raman spectra. When the pyrrolidine concentration reaches 0.12 M, two lines with almost the same intensities appear at 1347 and 1354 cm^{-1}. The 1347-cm^{-1} line was previously assigned as ν_4 of six-coordinate NiTPP.[30−34] As the pyrrolidine concentration increases, the intensity of ν_4 for $Ni(Pyr)_2TPP$ increases drastically, but the line at 1354 cm^{-1} increases very slowly. In addition, another new line at 1359 cm^{-1} grows at about the rate of the 1347-cm^{-1} line. This depolarized line at 1359 cm^{-1} has been assigned to ν_{29} (B_{2g}) of axially ligated NiTPP.[41] ν_{29} is typically a few wavenumbers higher than ν_4. When the pyrrolidine concentration increases further, only the two lines at 1347 and 1359 cm^{-1} can be seen, although the presence of the line at 1354 cm^{-1} is still evident in the filling-in between ν_{29} and ν_4 of the six-coordinate pyrrolidine complex.

The structure-sensitive line ν_2, composed mainly of $C_\beta-C_\beta$ stretching, occurs at 1573 cm^{-1} for four-coordinate NiTPP.[41] Of all the core-size marker lines, it is the least sensitive to core size (probably because of the low contribution of $C_\alpha-C_m$ stretching), comparable to the sensitivity of ν_4.[51] The variation of ν_2 with pyrrolidine concentration is shown in Figure 4c. In neat CH_2Cl_2, there are mainly three lines in the region from 1530 to 1660 cm^{-1}: a broad and asymmetric ν_2 line, a phenyl

in-plane mode ϕ_4 at 1602 cm^{-1}, and a weak ν_{19} line at 1552 cm^{-1}. Upon addition of pyrrolidine, ν_{19} is obscured by a new line at 1546 cm^{-1} that grows in at the expense of ν_2 of four-coordinate NiTPP. This polarized line corresponds to ν_2 of the six-coordinate complex in neat pyrrolidine (12 M)[52,53] and is much more narrow and symmetric than the line at 1573 cm^{-1}. The 1615-cm^{-1} line may be ν_{10} of the axially ligated species. Apparently, ϕ_4 downshifts three wavenumbers to 1599 cm^{-1} for the six-coordinate complex. The five-coordinate ν_2 line is not observed probably as a result of the spectral crowding in this region.

The low-frequency region from 200 to 600 cm^{-1} shown in Figure 4d usually serves as a fingerprint region for the peripheral substituents,[13] but it also contains ν_8, which while structure sensitive also depends on other factors. This macrocycle breathing mode consists primarily of Ni−N$_{pyrrole}$ and C$_\alpha$−C$_m$ bond stretching motion and methine bridge bending.[8] The ν_8 line for four-coordinate NiTPP appears around 40 cm^{-1} and is broad and asymmetric. When the pyrrolidine concentration increases to about 3 M, a shoulder appears on the low-frequency side of four-coordinate ν_8 and grows in at the highest concentrations as a sharp and symmetric line at 380 cm^{-1}. This line is assgned as ν_8 of the six-coordinate species. The small shoulder on the high-frequency side of the 380-cm^{-1} line might be the phenyl out-of-plane mode π_5. Two additional six-coordinate lines are found at 218 and 442 cm^{-1}. The band at 334 cm^{-1} for the four-coordinate species is probably the porphyrin out-of-plane A$_{1u}$ and mode γ_2.[41] This region of the spectrum also suffers from spectral crowding, and the weak five-coordinate ν_8 line is not observed.

UV−Visible Absorption Spectroscopy. The Soret band for four-coordinate NiTPP in CH_2Cl_2 is at 414 nm, and that for the axially ligated species is at 434 nm (inset in Figure 3).[30−34] Upon raising the pyrrolidine concentration, the band at 434 nm increases at the expense of the band of four-coordinate NiTPP (Figure S3). Unfortunately, no separate bands are seen for five- and six-coordinate species. Either only one form exists or both forms coexist but have similar band positions and shapes.

Figure 5 shows a plot of the absorption spectra changes at 408 nm as a function of total pyrrolidine concentration. Assuming there is only one coordinated form, the fit (not shown) to the absorption data is very poor and exhibits large systematic deviations. This could imply the coexistence of two ligated forms with equilibria expressed by

$$P + L \leftrightarrows PL, \qquad PL + L \leftrightarrows PL_2$$

with equilibrium constants K_1 and K_2, respectively. The coexistence of two ligated forms is also implied by the lack of a clear isosbestic point for the titration absorption spectra in Figure S3. The nonlinear least-squares fit to the data (solid line) gives $K_1 = 1.08$ M^{-1} and $K_2 = 3.79$ M^{-1}. The values of K_1 and K_2 are in reasonable agreement with the result obtained by Kim et al. for ligation of piperidine with Ni tetrakis(*p*-cyanophenyl)porphine.[34]

The upper inset in Figure 5 gives the mole fractions of the five- and six-coordinate species as a function of the total concentration of added pyrrolidine. The second ligand binds somewhat more strongly than the first so that little of the five-coordinate species is observed at any ligand concentration. The calculated maximum concentration of the five-coordinate complex is about 10%. The ratio of concentrations of the five- and six-coordinate complexes is shown in the lower inset in Figure 5. The ratio decreases with the total pyrrolidine concentration. There are almost equal amounts of five- and six-coordinate complex at about 0.2 M, where there is also enough of these coordinated species to be seen in the Raman spectrum (Figure 4a).

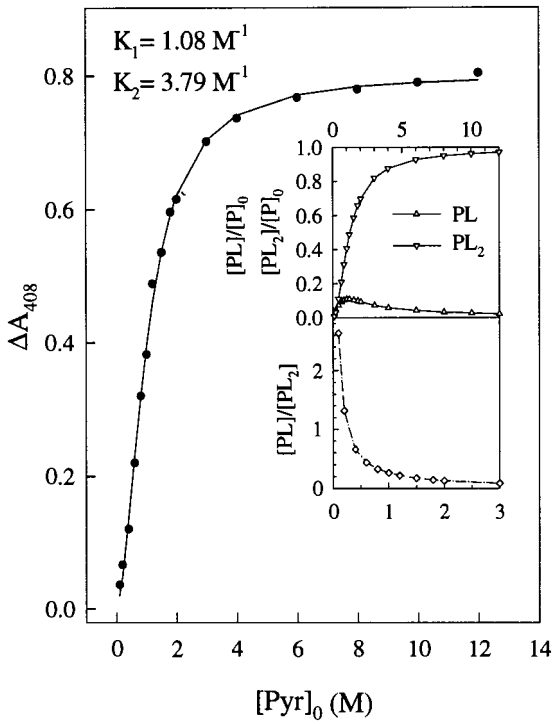

Figure 5. Curve-fit results of UV−visible spectra for NiTPP in dichloromethane with different pyrrolidine concentration. The upper inset: the concentration percentage of the five-coordinate and six-coordinate species versus the pyrrolidine concentration. The lower inset: dependence of the concentration ratio of the five- and six-coordinate species on pyrrolidine concentration.

Molecular Simulations. Molecular mechanics calculations were performed on NiTPP and its axially ligated complexes. The stable conformers (local minima) were found and the structural parameters for all the conformers are listed in Table 2. The calculated total energies and a breakdown of the various contributions to the total energy are given in Table 3.

For four-coordinate NiTPP, there are three stable conformers: purely ruffled, saddled, and planar, respectively. The ruffled one has the lowest energy. The saddled and planar forms are less than 1.8 kcal/mol (~3*RT* at room temperature) higher in energy than the ruffled one, and thus an equilibrium among these three conformers is established in solution. The coexistence of planar and nonplanar conformers for NiTPP in solution has been determined by temperature-dependent resonance Raman measurements.[19]

The calculated structure and the X-ray crystallographic structure of ruffled NiTPP match very well, especially for the macrocyclic atoms. Even without constraining the phenyl orientations to that determined by crystal packing, the Ni−N$_{pyrrole}$ distances are very close (1.924 Å for the crystal structure). The ruffling dihedral angles for the calculated and crystal structures are 30.7 and 27.9°, respectively (Table 2). Constraining the phenyl orientations gives even closer agreement, as can be seen from Figure 6a.

For five- and six-coordinate pyrrolidine complexes of NiTPP, conformers with many different axial ligand orientations are stable owing to the very small energy barrier for ligand rotation.

(52) Kim, D.; Kirmaier, C.; Holten, D. *Chem. Phys*. **1983**, *75*, 305.
(53) Kim, D.; Holten, D. *Chem. Phys. Lett.* **1983**, *98*, 584.

Table 2. Selected Average Structural Parameters Obtained from Calculated Conformations and Crystal Structures for NiTPP (a) and Its Axially Ligated Complexes (b)[a] (Bond Lengths in Å, Bond Angles in deg)

(a) Structural Parameters for NiTPP

porphyrin conformer		Ni−N	dihedral angle	$C_\alpha-N-C_\alpha$	N−Ni−N	$C_\beta-C_\beta$	$C_\alpha-C_m$	$C_\alpha-N$	$NC_\alpha-C_mC_\alpha$	$NC_\alpha-C_\beta C_\beta$
NiTPP	*ruf*	1.924	30.7	105.2	180.0	1.327	1.386	1.382	12.7	1.9
	sad	1.949	0.6	104.5	175.8	1.322	1.385	1.385	4.9	2.4
	planar	1.955	0.1	104.4	179.9	1.320	1.384	1.387	0.1	0.1
	crystal	1.929	27.9	105.0	178.7	1.357	1.384	1.380	7.2	2.4
	high-spin	2.042	0.4	107.4	180.0	1.331	1.400	1.380	0.2	0.0

(b) Structural Parameters for Axially Ligated Complexes of NiTPP

porphyrin conformer		Ni−N	Ni−N_{axial}	dihedral angle	$C_\alpha-N-C_\alpha$	N−Ni−N	$C_\beta-C_\beta$	$C_\alpha-C_m$	$C_\alpha-N$	$NC_\alpha-C_mC_\alpha$	$NC_\alpha-C_\beta C_\beta$	HN_{ax}−NiN
Ni(Pyr)TPP	0	2.044	2.129	1.3	107.3	175.9	1.331	1.400	1.380	2.8	1.1	0.0
	45	2.042	2.126	4.0	107.4	176.1	1.331	1.400	1.379	2.0	0.3	45.0
Ni(PiP)TPP	45	2.041	2.143	9.7	107.4	174.8	1.331	1.400	1.379	4.3	0.58	44.8
	0	2.043	2.157	1.0	107.3	173.6	1.331	1.400	1.379	2.1	1.2	0.3
Ni(Pyr)2TPP	0 perp	2.043	2.142	2.7	107.4	177.5	1.331	1.400	1.380	1.6	1.3	0.3
	45 perp	2.041	2.136	8.0	107.4	179.7	1.331	1.400	1.379	3.7	0.5	42.5
	0 para	2.044	2.149	2.8	107.4	180.0	1.331	1.400	1.380	0.6	0.5	0.4
	45 para	2.043	2.141	1.2	107.4	180.0	1.331	1.400	1.80	0.6	0.1	45.1
$Ni(Pip)_2TPP$	45 perp	2.036	2.158	16.2	107.6	179.9	1.333	1.401	1.378	1.6	1.3	45.0
	0 perp	2.039	2.179	2.1	107.5	175.2	1.332	1.401	1.379	3.3	2.0	0.0
	45 para	2.046	2.177	0.6	107.4	180.0	1.331	1.401	1.380	0.3	0.1	45.1
	0 para	2.045	2.200	1.9	107.4	180.0	1.331	1.400	1.380	0.4	0.3	0.0
	crystal	2.043	2.256	12.8	105.9	180.0	1.336	1.405	1.370	3.3	0.4	44.9

[a] "0" and "45" indicate N−H bond(s) of ligand(s) sit(s) above Ni−$N_{pyrrole}$ bond and between Ni−$N_{pyrrole}$ bonds, respectively; "perp" and "para" indicate that the mean planes of the two axial ligands are perpendicular or parallel to each other, respectively.

Table 3. Energies (in kcal mol^{-1}) of Energy-Minimized Stable Conformers for NiTPP and Its Axially Ligated Complexes

porphyrin conformer[a]		relative[b]	total	bonds	angles	torsions	inversions	VdW	electrost.
NiTPP	*ruf*	0	180.72	9.56	70.59	47.49	0.65	60.14	−7.71
	sad	1.69	182.41	11.74	72.25	41.38	0.25	64.45	−7.64
	planar	1.78	182.50	12.50	72.20	40.00	0.00	65.50	−7.63
	high-spin	n/a	175.40	1041	72.81	40.00	0.00	59.74	−7.57
Ni(Pyr)TPP	0	0	181.22	10.87	78.08	45.50	0.04	56.45	−9.73
	45	0.52	181.74	10.82	79.08	45.27	0.02	56.35	−9.81
Ni(Pip)TPP	45	0	181.92	11.95	76.53	41.32	0.06	61.16	−9.10
	0	1.16	183.08	12.17	77.00	40.85	0.08	61.94	−8.96
$Ni(Pyr)_2TPP$	0 perp	0	188.33	11.91	83.65	50.88	0.09	53.42	−11.62
	45 perp	0.91	189.24	11.68	85.72	50.57	0.05	52.96	−11.74
	0 para	0.64	188.97	12.15	83.01	50.72	0.10	54.44	−11.45
	45 para	1.34	189.67	11.83	85.58	50.02	0.01	53.91	−11.68
$Ni(Pip)_2TPP$	45 perp	0	189.82	14.50	80.04	43.26	0.16	62.44	−10.57
	0 perp	3.32	193.14	15.52	81.29	41.66	0.19	64.92	−10.44
	45 para	2.70	192.52	15.33	80.55	40.72	0.00	66.29	−10.37
	0 para	6.16	195.98	16.67	80.65	40.79	0.05	67.91	−10.09

[a] "0" and "45" indicate N−H bond(s) of ligand(s) sit(s) above Ni−$N_{pyrrole}$ bond and between Ni−$N_{pyrrole}$ bonds, respectively; "perp" and "para" mean two axial ligands are perpendicular or parallel to each other, respectively. [b] Energy related to the lowest-energy conformer.

In Table 2b are listed structural parameters for most of these conformers. For the five-coordinate species, the structure with the average plane of the ligand eclipising the Ni−$N_{pyrrole}$ bond has lowest energy (Figure 7a). However, the highest-energy structure with the ligand plane bisecting two adjacent Ni−$N_{pyrrole}$ bonds is only 0.5 kcal/mol higher. For the six-coordinate complexes, the lowest-energy structure is the one with the two ligands eclipsing the Ni−$N_{pyrrole}$ bonds and perpendicular to each other. The energy span for six-coordinate conformers is only 1.3 kcal/mol. Consequently, all these axially ligated conformers will coexist in solution. In spite of these different orientations of the axial ligands, the macrocycles of the six-coordinate conformers all possess very similar structural parameters, and the same is true for the five-coordinate conformers (Table 2b).

The structures of piperidine−NiTPP complexes were also calculated and the results are given in Tables 2 and 3. As for the pyrrolidine complexes, stable conformers with several different ligand orientations were found. In contrast with the pyrrolidine complexes, the lowest-energy structure for the five-coordinate piperidine−NiTPP complex is the one with the axial ligand bisecting two adjacent Ni−$N_{pyrrole}$ bonds. For the six-coordinate conformers with axial ligands at 45° to Ni−$N_{pyrrole}$ bonds, the one with the ligand planes perpendicular has the lowest energy.

For the crystal structure, the planes of the two axial ligands are antiparallel to each other and lie ∼45° between two Ni−$N_{pyrrole}$ bonds. However, this conformer is calculated to be only 2.7 kcal/mol higher than the lowest-energy configuration.

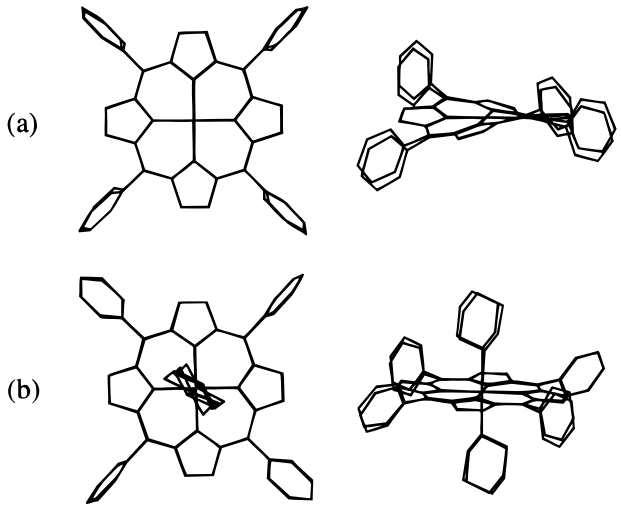

Figure 6. Side and top views for the comparison of X-ray crystal structures and calculated structures for NiTPP (a) and Ni(Pip)$_2$TPP (b).

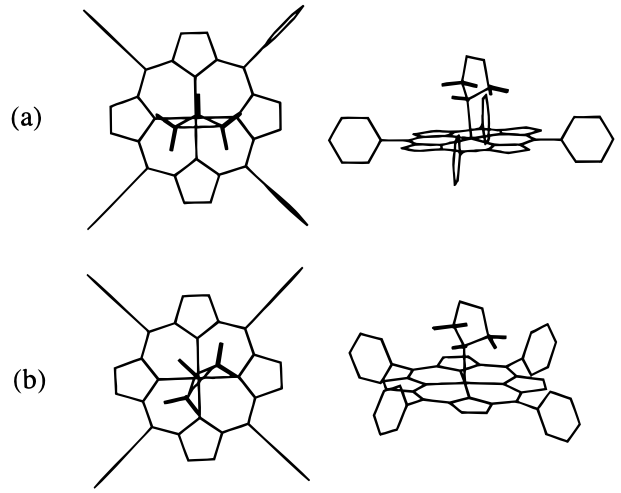

Figure 7. Illustrations of the orientations of axial ligand binding on NiTPP. (a) The plane of the axial ligand eclipses a Ni−N$_{porphyrin}$ bond; (b) the plane of the axial ligand lies ∼45° between two Ni-N$_{porphyrin}$ bonds.

Normal-Coordinate Structural Decomposition. Table 4 gives the results for quantitative decomposition of the out-of-plane distortion of each conformer into contributions from deformation along the lowest-frequency normal coordinates of each symmetry type. Since the frequency of the *pro* (A_{1u}) distortion is very high, the van der Waals interaction with the peripheral substituents, axial ligands, and adjacent molecules in the crystal usually do not provide enough energy to induce this deformation type.[22] In the present study, the contribution from pyrrole propellering is found to be zero in all the cases and thus is not shown in Table 4.

For four-coordinate NiTPP, the three stable conformers are almost purely ruffled, saddled, or planar, respectively (Table 4a). The total out-of-plane distortion for the *ruf* conformer is close to the total distortion of the macrocycle in the crystal structure. Unlike the calculated structure, however, the crystal structure has a significant contribution from saddling. The saddling might result from different orientations of the phenyl groups. Specifically, the phenyl groups for the calculated unconstrained structure are almost perpendicular to porphyrin macrocycle (Figure 6). For the crystal structure, however, the phenyl groups are twisted so that they are closer to the mean plane of the macrocycle. Constraining the dihedral angles $C_\alpha C_m C_{s1} C_{s2}$ of the phenyl groups to those found in the crystal structure, the saddling contribution for the calculated structure becomes significant (Table 4a). The observed orientations of the phenyl groups most likely result from the crystal packing forces, thus the observed saddling contribution probably results from crystal packing.

The effects of axial ligands on nonplanar distortion of the porphyrin macrocycle are most evident in the NSD results. Whether the axial ligand is pyrrolidine or piperidine, similar types of out-of-plane distortions are observed. However, the total distortion is composed of different contributions from the symmetric deformations because of the different ligand orientations (Table 4b). For the five-coordinate conformers with axial ligands eclipsing the Ni−N$_{pyrrole}$ bonds, the distortion is a combination of *sad* and *dom* deformations; with axial ligands lying at 45° to Ni−N$_{pyrrole}$ bonds *ruf* and *dom* are the major components. In addition, for five-coordinate complexes with a specific ligand, both stable conformers have similar total distortions.

For the six-coordinate species, two ligands perpendicular to each other cause larger distortion than when the two ligands are parallel. In the latter case, the porphyrin macrocycle is almost planar. In the cases for which the ligand planes are perpendicular to each other, the macrocycle is mainly saddled when planes eclipse the Ni−N$_{pyrrole}$ bonds, and the porphyrin is mainly ruffled when the ligands sit between the two Ni−N$_{pyrrole}$ bonds. It is worth mentioning that the degree of nonplanar distortion for the six-coordinate crystal structure, which has only *wav*(*x*) and *wav*(*y*) deformations, is very different from that for the calculated structure with same ligand orientation (45°, antiparallel). Like four-coordinate NiTPP, crystal packing forces might contribute to this difference. Indeed, constraining the peripheral phenyl groups to the same orientation as in the crystal structure leads to significant nonplanar distortion, especially in the *wav*(*x*) and *wav*(*y*) contributions.

Discussion

Nonplanar Distortions of NiTPP Induced by Axial Ligation. Nonplanar distortions of the porphyrin macrocycle are highly dependent on the central metal[23] and the peripheral substituents[13,22] including the pattern (i.e., number and position), size, shape, and orientation of the substituents. Planar Ni porphyrins are found in solution only when the peripheral substituents are hydrogen atoms (Ni(P)),[54] or when the steric constraints imposed by the substituents make in-plane distortion preferable (NiTC$_5$TPP).[20] All other Ni porphyrins in solution are either nonplanar or a mixture of nonplanar and planar forms, with nonplanar ones as the lowest-energy structures.[19−24,55−57] For four-coordinate NiTPP, resonance Raman spectroscopy has recently shown that at least two conformers coexist in solution: a nearly planar form and at least one nonplanar form.[19] MM calculations predict three stable conformers: *ruf*, *sad*, and planar, and there are no conformers containing *dom*, *wav*(*x*), or *wav*(*y*) contributions. The nonplanar conformers partly result from low-spin Ni being too small for the porphinato core. In the absence of axial ligands, only one nearly planar form is

(54) Jentzen, W.; Turowska-Tyrk, I.; Scheidt, W. R.; Shelnutt, J. A. *Inorg. Chem*. **1996**, *35*, 3559.
(55) Anderson, K. K.; Hobbs, J. D.; Luo, L.; Stanley, K. D.; Quirke, J. M. E.; Shelnutt, J. A. *J. Am. Chem. Soc*. **1993**, *115*, 12346.
(56) Alden, R. G.; Crawford, B. A.; Doolen, R.; Ondrias, M. R.; Shelnutt, J. A. *J. Am. Chem. Soc*. **1989**, *111*, 2070.
(57) Jentzen, W.; Unger, E.; Karvounis, G.; Shelnutt, J. A.; Dreybrodt, W.; Schweitzer-Stenner, R. *J. Phys. Chem*. **1996**, *100*, 14184.

Table 4. Displacement (in Å) along the Lowest-Frequency Out-of-Plane Normal Coordinates of the Macrocycle for the Calculated and Crystal Structures of NiTPP (a) and Its Axially Ligated Complexes (b);[a] the Lowest Energy Complex Is Listed First in Each Case

porphyrin conformer		total						
		observed	fit	*sad*	*ruf*	*dom*	*wav*(*x*)	*wav*(*y*)
				(a) Displacement in NiTPP				
NiTPP	low-spin	1.482	1.479	0.005	1.479	0.000	0.000	0.000
		1.091	1.090	1.090	−0.027	0.000	0.000	0.000
		0.023	0.023	0.023	0.003	0.000	0.000	0.000
	constrained phenyls[b]	1.550	1.547	0.350	1.507	0.000	0.000	0.000
	crystal	1.321	1.317	0.237	1.296	0.000	0.000	0.000
NiTPP	high-spin	0.018	0.018	0.000	0.018	0.000	0.000	0.000
				(b) Displacement in Axially Ligated Complexes of NiTPP				
Ni(Pyr)TPP	0	0.175	0.167	0.137	0.003	0.095	−0.005	0.000
	45	0.210	0.209	0.000	0.200	0.059	0.011	0.010
Ni(Pip)TPP	45	0.479	0.477	0.000	0.467	0.100	0.006	0.006
	0	0.517	0.515	0.503	0.013	0.111	0.011	0.000
$Ni(Pyr)_2TPP$	0 perp	0.233	0.221	0.221	−0.002	0.000	0.004	0.004
	45 perp	0.401	0.400	0.055	0.396	0.000	0.003	−0.017
	0 para	0.080	0.024	0.000	0.021	0.000	−0.011	0.000
	45 para	0.032	0.029	0.011	0.000	0.000	0.019	0.019
$Ni(Pip)_2TPP$	45 perp	0.448	0.448	−0.001	0.448	0.000	0.000	0.000
	0 perp	0.876	0.874	0.874	−0.007	0.000	0.018	0.017
	45 para	0.012	0.009	0.000	0.000	0.000	−0.007	0.005
	0 para	0.052	0.019	0.000	−0.006	0.000	0.000	0.018
	constrained phenyls[a]	0.123	0.114	0.052	0.033	−0.028	0.087	0.030
	crystal	0.342	0.259	0.000	0.000	0.000	0.215	0.144

[a] "0" and "45" indicate N-H bond(s) of ligand(s) sit(s) above $Ni-N_{pyrrole}$ bond and between $Ni-N_{pyrrole}$ bonds, respectively; "perp" and "para" indicate that the mean planes of the two axial ligands are perpendicular or parallel to each other, respectively. [b] Orientation of phenyl groups constrained.

calculated for high-spin NiTPP owing to the expansion of the porphyrin core resulting from the promotion of an electron to $d_{x^2-y^2}$. Octaethylporphyrin might have provided a better model of biological porphyrins than TPP, but the out-of-plane distortions of the two porphyrins are similar, showing a similar mixture of planar and nonplanar forms in solution.

The axial ligands of high-spin Ni porphyrins cause nonplanar distortions of the macrocycle. Among the four types of symmetric nonplanar distortions, a small core (low spin Ni) favors *ruf* and *sad* deformations and a large core (high spin Ni) favors *dom* and *wav* deformations or a planar conformation.[23] Accordingly, while the low-spin NiTPP crystal structure shows a total nonplanar displacement of 1.321 Å contributed by mainly *ruf* and *sad* deformations (Table 4a), the crystal structure of high-spin $Ni(Pip)_2TPP$ shows a total displacement of only 0.342 Å, composed of *wav*(*x*) and *wav*(*y*) deformations only. High-spin four-coordinate NiTPP is calculated to be nearly planar; therefore, axial ligation and crystal packing forces induce the *wav* deformation. In fact, the antiparallel relative orientation of the two ligands has the proper symmetry to induce *wav* deformation.

Medforth et al. have studied axial ligand orientations in highly nonplanar porphyrins and conclude that the porphyrin conformation influences the orientations of axial ligands.[58,59] For highly distorted porphyrins like Co^{III}OETPP or Co^{III}T(tBu)P, the addition of axial ligands does not change the conformation of the porphyrin macrocyle. The planes of the axial ligands are oriented approximately parallel to the cavities formed by the nonplanar porphyrin macrocycle. Specifically, for the structure Co^{III}OETPP, which has a *sad* conformation, the planes of the axial ligands nearly eclipse the $Co-N_{pyrrole}$ bond and are perpendicular to each other. For Co^{III}T(tBu)P, which has a *ruf* structure, the planes of the axial ligands bisect the $Co-N_{pyrrole}$ bonds and are also perpendicular to each other.

For high-spin NiTPP, nearly planar conformers are predicted by MM. No groove for the ligands is formed as in the case of Co^{III}OETPP or Co^{III}T(tBu)P for which large distortions are caused by severe steric crowding. Therefore, the orientations of the axial ligands of NiTPP are not substantially confined by the porphyrin. However, the ligands may take several orientations and induce distinctive distortions of the porphyrin macrocycle as a result (Table 4). For five-coordinate species, the eclipsed and 45° complexes have similar total out-of-plane displacements, and the main contributions are either *sad* and *dom* or *ruf* and *dom*, respectively. Of course, the *dom* distortion occurs because the axial ligand pulls the metal out of the mean plane. The orientation of the ligand (Figure 7) determines the symmetry of the interaction between the ligand and the porphyrin (B_{2u} and B_{1u}) leading to a saddling or ruffling contribution. As expected the ligand-induced distortion is large for the six-membered ring than the five-membered ring. In addition, the interaction between the hydrogen atom on the ligand nitrogen and the porphyrin ring, introduces additional asymmetry that appears as a wave contribution. The degree of wave distortion is much smaller than saddling, partly because the frequency of the waving deformation is much higher than for saddling and ruffling (Figure 1), and, consequently, much more energy is required to cause a significant distortion.[22] These steric interactions between the ligand and porphyrin are not completely symmetric as evidenced by the very small ruffling.

MM calculations for six-coordinate NiTPP complexes predict four stable conformers (Tables 1−3). No doming distortion is found owing to almost equal and opposite steric interactions with the two axial ligands. Similarly, in the case of two parallel ligands, the porphyrin macrocycle is much less distorted because

(58) Medforth, C. J.; Muzzi, C. M.; Shea, K. M.; Smith, K. M.; Abraham, R. J.; Jia, S.; Shelnutt, J. A. *J. Chem. Soc., Perkin Trans. 2* **1997**, 833.
(59) Medforth, C. J.; Muzzi, C. M.; Shea, K. M.; Smith, K. M.; Abraham, R. J.; Jia, S.; Shelnutt, J. A. *J. Chem. Soc., Perkin Trans. 2* **1997**, 839.

of increased symmetry and the cancellation of the steric interactions of the ligands on different sides of porphyrin macrocycle. In addition, the two $N_{ligand}-H$ hydrogens interact with the porphyrin macrocycle to give either *wav*(*x*), *wav*(*y*), or equal *wav*(*x*) and *wav*(*y*) distortions depending on the relative orientations of the ligands.

Five-Coordinate NiTPP. The nickel(II) ion, bound to a square-planar tetradentate ligand such as a porphyrin, is normally found in the spin-zero (low-spin) in which the d orbitals of nickel are completely filled except for the $d_{x^2-y^2}$ orbital.[60] The highest-energy filled orbital is the d_{z^2}. In the high-spin ($S = 1$) state, an electron in the d_{z^2} orbital is promoted to the $d_{x^2-y^2}$ orbital, leaving a half-filled d_{z^2} orbital, which can accept charge from either one or two σ-donating axial ligands. In the coordination of NiTPP to basic ligands such as pyrrolidine, imidazole, and piperidine, NiTPP forms mainly six-coordinate complexes[30−32,52,53,61,62] although a five-coordinate species has been introduced in some cases to better explain spectral changes with ligand concentration. However, no unique absorption or resonance Raman spectral features have been directly observed for the five-coordinate complex. Kim et al.[33,34] studied the coordination of NiTPP with piperidine and claimed that ν_{28} (B_{2g}) at 1356 cm^{-1} in the resonance Raman spectra is partially contributed by ν_4 of the five-coordinate complex. This claim was based on a decrease in the depolarization of ν_4 from 0.75 to 0.53. However, they did not observe a resolved ν_4 line for five-coordinate NiTPP.

By precisely varying the pyrrolidine concentration, we have obtained direct evidence for the existence of five-coordinate NiTPP in the ν_4 region of the resonance Raman spectra. At low pyrrolidine concentration (0.1−0.6 M), a line is observed at 1354 cm^{-1} (Figure 4a), and like ν_4 of the four-coordinate (1373 cm^{-1}) and six-coordinate (1346 cm^{-1}) complexes, the line is polarized and thus could be ν_4 of the five-coordinate form. This intermediate frequency is reasonable since the five-coordinate complex is expected to be high spin.[33,63] Typically, promotion of a d_{z^2} electron into the antibonding $d_{x^2-y^2}$ orbital results in a large change in the porphyrin core size and Ni−N bond length. For example, the five-coordinate histidine complex in Ni-reconstituted hemoglobin also has frequencies for the core-size marker lines that are intermediate between four- and six-coordinate species. In addition, the d−d transition (without axial coordination) is observed in transient Raman spectra, and the frequency of ν_4 in the d−d excited state is also intermediate between four- and six-coordinate complexes.

When the pyrrolidine concentration is 0.12 M, the Raman line at 1354 cm^{-1} is at almost the same height as the line at 1347 cm^{-1}, indicating significant concentrations of the five-coordinate complex, especially since the excitation wavelength is not at resonance with the coordinated species. In addition, the amount of the six-coordinate form increases much faster than the five-coordinate form, as predicted for the concentration ratio of five-coordinate to six-coordinate species (inset, Figure 5). The Ni−ligand vibration mode for the five-coordinate species could not be identified in the low-frequency region of the Raman spectra as it was for the Ni−histidine stretch (observed at 236 cm^{-1}) in five-coordinate nickel-reconstituted hemoglobin.[64] This is likely a consequence of the low concentration of the NiTPP five-coordinate species.

In contrast with these Raman results, Soret bands for the five- and six-coordinate NiTPP complexes are not resolved at any pyrrolidine concentration. However, the change in absorption as a function of ligand concentration requires different equilibria for the five- and six-coordinate complexes thus indirectly indicating the presence of the five-coordinate form.

Macrocyclic Conformational Heterogeneity and Axial Ligation. Until recently,[19] NiTPP was thought to be planar in solution. However, based on line-shape analysis of two structure-sensitive lines, ν_2 and ν_8, which are very broad (FWHM ~16 cm^{-1}) and asymmetric, it was shown that more than one conformer is present (Figures 3 and 4). This detailed study using crystallography, resonance Raman spectroscopy, and molecular mechanics calculations[19] concludes that an equilibrium exists between the nonplanar and planar conformers and that the enthalpies of the conformers differ by less than 2.5 kJ/mol.

Upon coordination of axial ligand(s), the Raman lines ν_2 and ν_8 for NiTPP become narrow (~8 cm^{-1}) and symmetric (Figures 3 and 4). This might imply that there exists only one axially ligated conformer. On the other hand, molecular mechanics calculations for the pyrrolidine−NiTPP complexes predict many conformers with differing ligand orientations for five- and six-coordinate species (Table 2b). The energy differences for the five-coordinate conformers are less than *RT* (at room temperatures) and for the six-coordinate species are less than 2RT (Table 3). However, regardless of the orientation of the pyrrolidine ligand(s), the bond distances of $C_\beta-C_\beta$, $C_\alpha-C_m$, and $C_\alpha-N$ are almost same for all the conformers. In addition, the Ni−N distance varies within ±0.002 Å, and the ruffling dihedral angles range from 1.2 to 8.0°. Thus, the question is whether these small structural differences could result in any observable shift of the structure-sensitive Raman lines since these lines are dependent on both the porphyrin core size and nonplanarity. In particular, an increase in core size of 0.002 Å results in a decrease in frequency of approximately 1 cm^{-1} for ν_2.[65,66] Therefore, the variation in core size for all the conformers would lead to a frequency variation of no more than 1 cm^{-1}. Similarly, the frequencies of the structure-sensitive marker lines have only weak dependence on ruffling angle for small angles and, thus, the variation in ruffling dihedral angle from 1.2 to 8.0° is not enough to cause measurable shifts in Raman frequencies for the structure-sensitive lines.[13,22] While the MM calculations show significant variations in the macrocyclic conformation for the axially coordinated species, spectroscopic probes are particularly insensitive to nonplanar distortions for the near-planar conformers predicted, and therefore, the structural heterogeneity cannot be observed. This conclusion is consistent with NMR results showing that non-sterically hindered axial ligands rotate rapidly, even at −95 °C.[67] Thus, evidence for only one five-coordinate and one six-coordinate form is found, and the structure-sensitive lines ν_2 and ν_8 for the axially ligated NiTPP have widths consistent with only one conformer.

Orientation of the Axial Ligands. It is believed that different orientations of the axial histidine ligands might be one mechanism for altering the oxidation potentials and spectroscopic properties of cytochromes.[15−18] For example, the imidazole rings of the two coordinated histidines in cytochromes

(60) Shelnutt, J. A. *J. Phys. Chem*. **1989**, *93*, 6283.
(61) Walker, F. A.; Hui, E.; Walker, J. M. *J. Am. Chem. Soc*. **1975**, *97*, 2390.
(62) MacCragh, A.; Storm, C. B.; Koski, W. S. *J. Am. Chem. Soc*. **1965**, *87*, 1470.
(63) Ake, R. L.; Gouterman, M. *Theor. Chim. Acta* **1970**, *17*, 408.
(64) Shelnutt, J. A.; Alston, K.; Ho, J.-Y.; Yu, N.-T.; Yamamoto, T.; Rifkind, J. M. *Biochemistry* **1986**, *25*, 620.
(65) Spiro, T. G. In *Iron Porphyrin*, Part II; Lever, A. B. P., Gray, H. B., Eds.; Addison-Wesley: Reading, MA, 1982; p 89.
(66) Shelnutt, J. A. *J. Am. Chem. Soc*. **1987**, *109*, 4169.
(67) Walker, F. A.; Simonis, U. *J. Am. Chem. Soc*. **1991**, *113*, 8652.

b_5 and three of the four hemes of cytochromes c_3 are almost parallel.[68,69] The other heme in the cytochromes c_3 has its imidazole rings in nearly perpendicular planes. Furthermore, based on studies of a series of model compounds, Safo and coworkers suggested that the relative orientation of the axial ligands is related to the configuration of the Fe atom, which strongly depends on the π-accepting character and basicity of the ligand.[18] If the ligand has low basicity or the π-accepting character of the ligand dominates, then an unusual $(d_{xz},d_{yz})^4(d_{xy})^1$ configuration results and the perpendicular orientation of the ligands is observed. High basicity or strong π-donating character leads to parallel ligands. This is also true for other metalloporphyrins. For example, the complexes of Co(II) and Co(III) porphyrins with axial ligands like piperidine or imidazole are found to adopt an orientation in which the two axial ligands are parallel to each other and bisect the metal−nitrogen bonds.[36−38]

A parallel ligand orientation is also observed for nickel porphyrin complexes such as $NiTMPyP(Im)_2$[45] and $NiTPP(Pip)_2$ in this work. However, the MM calculations predict that the lowest-energy structure for $NiTPP(Pip)_2$ has the perpendicular ligand orientation. This discrepancy in the prediction of the ligand orientation may partially be a result of crystal packing. Moreover, it is important to remember that the calculations omit any electronic interactions that favor one orientation over another because the torsion about the $Ni-N_{ligand}$ bond is assumed to be zero. The predicted relative stabilities of the different conformers may be reversed if this torsion parameter is nonzero. However, it is interesting that in the protein environment such as for the cytochromes c_3, no particular preference for one orientation over the other is found and both parallel and perpendicular orientations are observed.

Conclusions

In strongly coordinating solvents like pyrrolidine, NiTPP forms five-coordinate as well as six-coordinate complexes that can be monitored directly by resonance Raman spectroscopy. Although the absorption band for five-coordinate species is not resolved from six-coordinate species, a distinct ν_4 Raman line is observed. Based on Raman line intensities, the proportion of five-coordinate species varies with ligand concentration, with a maximum of about 10% at 0.2 M pyrrolidine. From the Raman results, obvious macrocyclic conformational heterogeneity exists for four-coordinate NiTPP, but apparent homogeneity exists for the six-coordinate pyrrolidine complex because of the similarity in macrocycle structures and lack of sensitivity of the structural marker lines. Nevertheless, MM calculation suggests that conformers with several ligand orientations and different nonplanar distortions probably coexist in solution for both the five- and six-coordinate species. Apparently, the ligand-dependent conformers are undetectable spectroscopically, even though MM calculations indicate that the distortion for some of the conformers is as large as 0.9 Å.

The implications of these results are first that ligand orientation probably plays only a minor role in causing the large heme distortions observed in some heme proteins. The *c*-type cytochromes and the peroxidases in particular exhibit conserved nonplanar distortions, larger than 1 Å for some protein crystal structures. The pyrrolidine complexes are probably better models for the 5-membered imidazole ring, thus on the basis of the present results, ligand-induced distortions should not be greater than 0.4 Å (Table 4). Actually, the effect is probably no more than 0.2 Å for five-coordinate complexes, and only reaches 0.4 Å for six-coordinate complexes when the ligands are nearly perpendicular to each other. These conclusions are based on MM calculations, but Raman spectroscopic methods would detect ligand-induced nonplanar distortions if they were much larger than those predicted by the calculations. Thus, the large out-of-plane distortions that are observed in some protein crystal structures are the result of a combination of ligand-induced distortion with additional protein−heme interactions.

Supporting Information Available: Tables S1−S6 list X-ray crystal structural data for bis(piperidine) Ni(II) tetraphenylporphyrin; Figure S1 is the top view of $NiTPP(Pip)_2$. Figure S2 shows the 24-atom mean plane for $NiTPP(Pip)_2$; Figure S3 shows the UV−visible absorption spectra for NiTPP in CH_2Cl_2 titrated with pyrrolidine (10 pages). Ordering information is given on any current masthead page.

IC980289+

(68) Pierrot, M.; Haser, R.; Frey, M.; Payan, F.; Astier, J.-P. *J. Biol. Chem.* **1982**, *257*, 14341.
(69) Higuchi, Y.; Kusunoki, M.; Matsuura, Y.; Yasuoka, N.; Kakudo, M. *J. Biol. Chem.* **1984**, *172*, 109.